Chapter 21
Mid-infrared Laser Based Gas Sensor Technologies for Environmental Monitoring, Medical Diagnostics, Industrial and Security Applications

Frank K. Tittel, Rafał Lewicki, Mohammad Jahjah, Briana Foxworth, Yufei Ma, Lei Dong, Robert Griffin, Karol Krzempek, Przemyslaw Stefanski, and Jan Tarka

Abstract Recent advances in the development of compact sensors based on mid-infrared continuous wave (CW), thermoelectrically cooled (TEC) and room temperature operated quantum cascade lasers (QCLs) for the detection, quantification and monitoring of trace gas species and their applications in environmental and industrial process analysis will be reported. These sensors employ a 2*f* wavelength modulation (WM) technique based on quartz enhanced photoacoustic spectroscopy (QEPAS) that achieves detection sensitivity at the ppbv and sub ppbv concentration levels. The merits of QEPAS include an ultra-compact, rugged sensing module, with wide dynamic range and immunity to environmental acoustic noise. QCLs are convenient QEPAS excitation sources that permit the targeting of strong fundamental rotational-vibrational transitions which are one to two orders of magnitude more intense in the mid-infrared than overtone transitions in the near infrared spectral region.

Keywords Laser spectroscopy • Quartz enhanced photoacoustic spectroscopy • Wavelength modulation spectroscopy • Quantum cascade lasers • Trace gas detection • Carbon monoxide • Nitric oxide

F.K. Tittel (✉) • R. Lewicki • M. Jahjah • B. Foxworth • Y. Ma
Department of Electrical and Computer Engineering, Rice University,
6100 Main Street, Houston, TX 77005, USA
e-mail: fkt@rice.edu

L. Dong • R. Griffin
Department of Civil and Environment Engineering, Rice University,
6100 Main Street, Houston, TX 77005, USA

K. Krzempek • P. Stefanski • J. Tarka
Laser and Fiber Electronics Group, Wroclaw University of Technology,
Wybrzeze Wyspianskiego 27, 50-370 Wroclaw, Poland

M.F. Pereira and O. Shulika (eds.), *Terahertz and Mid Infrared Radiation: Detection of Explosives and CBRN (Using Terahertz)*, NATO Science for Peace and Security Series B: Physics and Biophysics, DOI 10.1007/978-94-017-8572-3_21,

21.1 Introduction

The development of compact trace gas sensors, in particular based on quantum cascade (QC) lasers, permit the targeting of strong fundamental rotational-vibrational transitions in the mid-infrared that are one to two orders of magnitude more intense than overtone transitions in the near infrared. The architecture and performance of three sensitive, selective and real-time gas sensor systems based on mid-infrared semiconductor lasers will be described [1–4]. A QEPAS based sensor capable of ppbv level detection of CO, a major air pollutant, was developed. We used a 4.61 μm high power CW DFB QCL that emits a maximum optical power of more than 1 W in a continuous-wave (CW) operating mode [3, 5, 6]. For the R(6) CO line, located at 2,169.2 cm^{-1}, noise-equivalent sensitivity (NES, 1σ) of 2 ppbv was achieved at atmospheric pressure with a 1 s data acquisition time. Furthermore, a high performance (>100 mW) 5.26 μm CW TEC DFB-QCL (mounted in a high heat load (HHL) package) based QEPAS sensor for atmospheric NO detection will be reported [7, 8]. A 1σ minimum detection limit of 3 ppbv was achieved for a sampling time of 1 s using interference free NO absorption line located at 1,900.08 cm^{-1}.

21.2 Quartz Enhanced Photo-Acoustic Spectroscopy (QEPAS)

In this work we selected quartz-enhanced photoacoustic spectroscopy (QEPAS), a gas-sensing technique first reported in 2002 by our Rice University Laser Science Group [9, 10]. The QEPAS sensor technology allows performing sensitive trace gas measurements in gas samples of a few mm^3 in volume. QEPAS employs readily available quartz tuning forks (QTFs) as sharply resonant acoustic transducers, instead of broadband electric microphones used in conventional photoacoustic spectroscopy sensor systems. The QTF is a piezo-electric element, capable of detecting weak acoustic waves generated when the modulated optical radiation interacts with a trace gas. The mechanical deformation of the QTF due to interaction with the acoustic waves results in the generation of electrical charges on its electrode pairs deposited on the prongs of the QTF. In order to further enhance the QEPAS signal, a so-called micro-resonator (mR) can be added to the QTF sensor architecture. The mR typically consists of two metal tubes [10, 11]. The QTF is positioned between the tubes to probe the acoustic waves excited in the gas contained inside the mR. To date, such a configuration has been used in most reported QEPAS based gas sensors [12, 13]. A recent optimization study revealed that for a 32 kHz QTF, two 4.4 mm-long tubes with 0.5–0.6 mm inner diameter yields the highest QEPAS signal-to-noise ratio (SNR) [11]. However to simplify optical alignment process and eliminate any potential optical fringes the 4 mm long tubes with 0.8 mm inner diameter are commonly used for QEPAS experiments in the mid-infrared region.

21.3 QEPAS Based ppb-Level Detection of Carbon Monoxide

21.3.1 Motivation for CO Detection

Carbon monoxide (CO), one of the major air pollutants in the United States, is mainly produced and released into the atmosphere by a variety of incomplete combustion activities, including the burning of natural gas, fossil fuel, and other carbon containing fuels. CO has an important impact on the atmospheric chemistry through its reaction with hydroxyl (OH) for troposphere ozone formation and also can affect the concentration level of greenhouse gases [13–15]. Furthermore, CO even at low concentration levels is dangerous to human life and therefore must be accurately and precisely monitored in real time.

21.3.2 CW DFB-QCL Based QEPAS Sensor System

A schematic of the QEPAS based CO sensor platform is shown in Fig. 21.1. As an excitation source a 4.61 μm high power, continuous wave (CW), distributed feedback quantum cascade laser (DFB-QCL) operating at 10 °C from Northwestern University [2, 5, 6] was employed. An external water cooling system was used to remove the heat dissipation from the hot surface of a TEC mounted in a commercial QCL housing (ILX Lightwave Model LDM-4872). The DFB-QCL beam is collimated

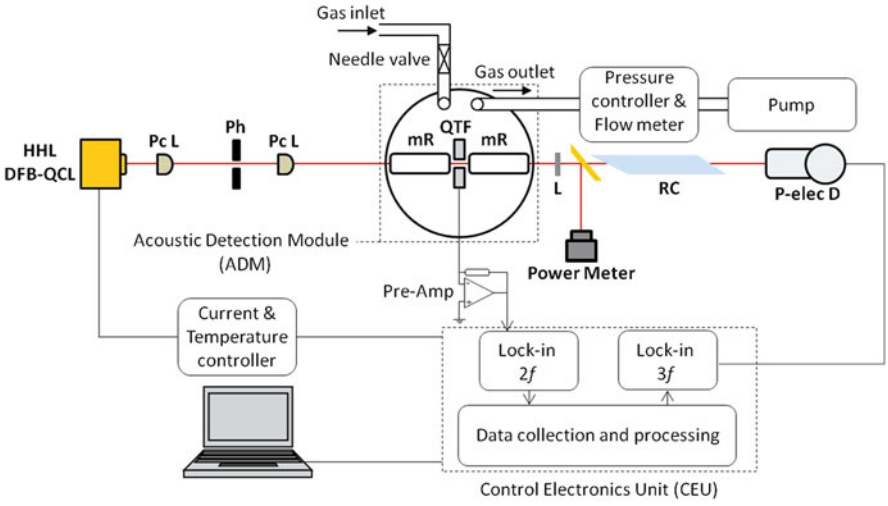

Fig. 21.1 Schematic configuration of a high power 4.61 μm CW RT TEC DFB-QCL based QEPAS system for CO and N_2O ppbv level detection. *Pc L* plano-convex lens, *Ph* pinhole, *QTF* quartz tuning fork, *mR* acoustic micro-resonator, *RC* reference cell

using a black diamond antireflection coated aspheric lens optimized for 3–5 μm spectral region with a 1.7 mm effective focal length (Lightpath model 390037-IR3). In order to further improve the QCL beam quality two additional 50 mm and 40 mm focal length plano-convex CaF_2 lenses, L_1 and L_2, and a pinhole with diameter of 200 μm as a spatial filter were used. The second lens L_2 was used to direct the laser beam through the mR and the gap between prongs of the QTF, located inside an acoustic detection module (ADM), with a transmission efficiency of >93 %. A ZnSe wedged window acting as a beam splitter (BS) is placed after the ADM to reflect ~20 % of the DFB-QCL beam into a gas reference channel. The rest of the high power CW DFB-QCL beam is delivered to an optical power meter (Ophir model 3A-SH) and used for alignment verification of the QEPAS system. A 3*f* reference channel signal is employed for locking of the QCL laser frequency to the peak of absorption line of the target analyte. In the reference channel the QCL beam is detected by a pyroelectric detector (InfraTec model LIE-332f-63) after passing through a reference gas cell. For precise and accurate CO concentration measurements, a 5 cm long reference gas cell filled with a 500 ppm CO:N_2 mixture at 150 Torr pressure (fabricated by Wavelength References, Inc) was used.

To improve the CO vibrational-translational relaxation processes an external humidifier was added at the inlet to the ADM of the QEPAS sensor system. In this case the addition of a 2.6 % H_2O vapor concentration to the target trace gas mixture acts as an effective catalyst and results in higher detected amplitude for CO and N_2O. A needle valve and flow meter (Brandt Instruments, Inc., Type 520) were used to set and monitor the gas flow through the QEPAS sensor system at a constant rate of 140 ml/min. A pressure controller (MKS Instruments, Inc., Type 649) and a vacuum pump were employed to control and maintain the pressure in the sensor system. The DFB-QCL current and temperature were set and controlled by an ILX Lightwave current source (model LDX 3220) and a Wavelength Electronics temperature controller (model MPT10000), respectively. For sensitive CO concentration measurements wavelength modulation spectroscopy (WMS) with 2nd harmonic detection [10, 11] was utilized. Modulation of the laser current was performed by applying a sinusoidal dither to the direct current ramp of the DFB-QCL at half of the QTF resonance frequency ($f=f_0/2 \sim 16.3$ kHz). The piezoelectric signal generated by the QTF was detected by a low noise trans-impedance amplifier with a 10 MΩ feedback resistor and converted into a voltage. Subsequently this voltage was transferred to a custom built control electronics unit (CEU). The CEU provides the following three functions: (1) measurement of the QTF parameters, i.e. the quality factor Q, dynamic resistance R, and the resonant frequency f_0; (2) modulation of the laser current at the frequency $f=f_0/2$; and (3) measurements of the 2*f* and 3*f* harmonic components generated by the QTF.

21.3.3 Performance of a 4.6 μm CW TEC DFB-QCL

The optical power emitted by the DFB-QCL operating at 1,250 mA current and 10 °C temperature is 987 mW in the CW operating mode (see Fig. 21.2a).

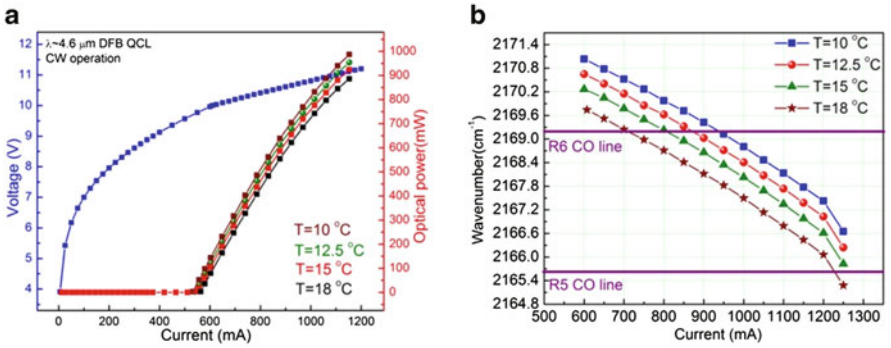

Fig. 21.2 (**a**) LIV curve of a 4.61 μm RT, CW, DFB-QCL from Center for Quantum Devices, Northwestern University; (**b**) DFB-QCL current tuning at different operating temperatures

The experimentally determined temperature and current tuning coefficients are –0.16 cm^{-1}/°C and –0.0065 cm^{-1}/mA, respectively. This DFB-QCL can be current tuned to target the R(5) and R(6) absorption lines of the ν_1 CO fundamental band at 2,165.6 cm^{-1} and 2,169.2 cm^{-1}, respectively (see Fig. 21.2b).

21.4 Experimental Details

21.4.1 Selection of CO and N_2O Spectrum Absorption Line

Quantitative measurements of CO in the ν_1 fundamental rotational-vibrational band were reported previously by several research groups [13, 15–17]. In Ref. [13] CO detection was performed using the R(8) CO absorption line located at 2,176.3 cm^{-1} by employing a Daylight Solutions, Inc external cavity quantum cascade laser (EC-QCL) based QEPAS sensor system. This CO sensor was operating at a reduced gas pressure of 100 Torr in order to avoid partial overlap with neighboring nitrous oxide (N_2O) line. In Ref. [16] the authors targeted the R(12) CO absorption line located at 2,190.0 cm^{-1} which has a small spectral overlap N_2O. However the R(12) line does not have a high absorption line intensity compared to other CO lines of the R branch [18]. In this work the R(6) CO absorption line located at 2,169.2 cm^{-1} was selected in order to measure the CO concentration with high accuracy and detection sensitivity.

To assess potential interferences from other atmospheric species, HITRAN based spectra of CO, N_2O, and H_2O absorption lines near 2,169 cm^{-1} were simulated at atmospheric pressure (760 Torr) and depicted in Fig. 21.3a. From simulated 2nd harmonic absorption spectra (Fig. 21.3b) it is clear that the R(6) CO line is free from spectral interference and can be used effectively in wavelength modulation spectroscopy of CO. Furthermore, the R(6) is one of the strongest line in the CO v_1 vibrational band with a 1.54 times higher absorption line intensity than for the R(12) line. For N_2O concentration measurements, an interference-free P(41) N_2O

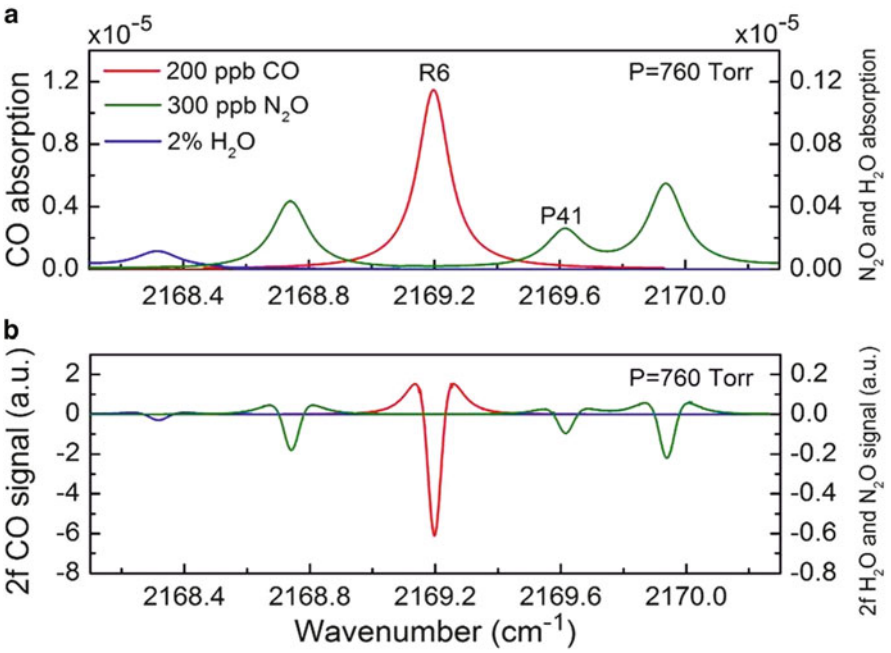

Fig. 21.3 HITRAN based simulation spectra of CO and N_2O at a temperature of 296 K, a standard atmospheric pressure, an optical path length of 1 cm for 200 ppbv CO, 2 % H_2O and 300 ppbv N_2O, respectively. (**a**): absorption spectra; (**b**): Second harmonic absorption spectra

absorption line located at 2,169.6 cm^{-1} was selected at a gas pressure of 100 Torr. The optical power measured after the ADM was 400 mW near 2,169 cm^{-1} for the CW DFB-QCL operating at 10 °C. The high QCL power helps to improve the QEPAS signal (S_0), which is proportional to: $S_0 \sim (\alpha \cdot P \cdot Q)/f_0$ where α is the absorption coefficient, P is the optical power, Q is the quality factor of the resonator and f_0 is the resonant frequency.

21.4.2 Line Locking for Continuous Monitoring of CO and N_2O Concentration Levels

Continuous monitoring of CO and N_2O concentration levels and the evaluation of the long term sensor performance of the QEPAS based sensor system was performed in the line locking mode, where the CW DFB-QCL frequency is kept at the center of the targeted absorption line. For line-locked measurements of the CO concentration at atmospheric pressure the modulation depth decreased from an optimum value of 50 mA to 40 mA because the 3*f* reference signal shape for the QEPAS sensor operating at 760 Torr is pressure broadened. The sealed CO reference cell was filled at a total pressure of 150 Torr.

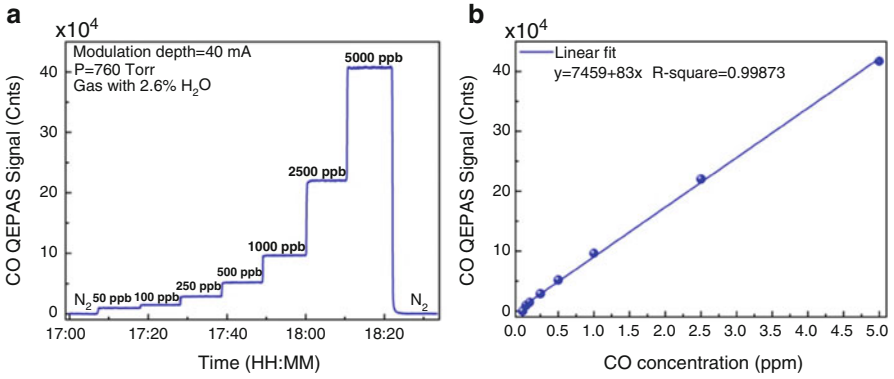

Fig. 21.4 (**a**) QEPAS signal amplitude recorded in the line locking mode as the CO concentration is varied at atmospheric pressure and a modulation depth of 40 mA. (**b**): QEPAS signals amplitude averaged from Fig. 21.4a as a function of CO concentration. 1cnt = 6.67×10^{-16} A

To verify the linear response of the mid-infrared QEPAS based CO sensor platform a calibration mixture of 5 ppmv CO:N_2 containing a constant 2.6 % concentration of water vapor was diluted six times down to 50 ppbv CO concentration levels (Fig. 21.4a). The data acquisition time for these measurements was set to 1 s.

The measured QEPAS signal amplitude as a function of CO concentration, is plotted in Fig. 21.4b. The calculated R-square value, which represents how well the regression line approximates real data points, is equal to ~0.999 after a linear fitting procedure. This implies that the sensor system exhibits a good linearity response to monitored CO concentration levels. However, due to the decrease of the modulation depth to 40 mA, the measured signal amplitude of moisturized 5 ppmv CO: N_2 mixture is 22 % lower compared to the line scanning mode experiments if a 50 mA modulation depth is used. Based on the data in Fig. 21.4a, the calculated MDL is 1.9 ppbv which is in good agreement with the MDL value that was calculated for the QEPAS sensor operated in the scanning mode. The re-calculated NNEA coefficient in this case is 2.04×10^{-8} cm^{-1} $W/\sqrt{Hz}$.

To evaluate the N_2O QEPAS sensor performance similar measurements were carried out by targeting the P(41) N_2O absorption line using a certified mixture of 1.8 ppmv N_2O:N_2. The optimum signal level was obtained when the gas pressure and modulation depth were set to 100 Torr and 20 mA, respectively. The addition of a 2.6 % H_2O concentration to the analyzed N_2O:N_2 mixture resulted in a fivefold enhancement of QEPAS signal amplitude and resulted in a MDL of 23 ppbv. The corresponding NNEA coefficient was found to be 2.91×10^{-9} cm^{-1} $W/\sqrt{Hz}$.

To investigate the long term stability and precision of the CO QEPAS sensor an Allan deviation analysis was performed by passing pure N_2 through the sensor system. From the Allan deviation plot shown in Fig. 21.5 the optimum averaging time for the CO sensor is found to be 500 s, which results in a MDL of 280 pptv. A similar Allan deviation analysis was also performed for the N_2O QEPAS sensor

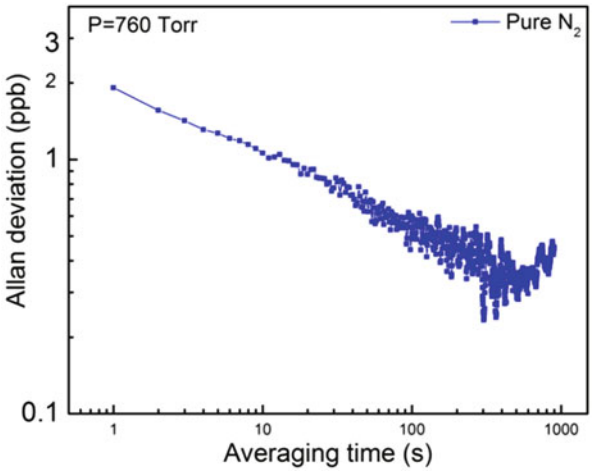

Fig. 21.5 Allan deviation plot for time series measurements of pure N_2 for the QEPAS based CO sensor system

when the laser wavelength was locked to the P(41) N_2O absorption line. In this case, after averaging the acquired data for 500 s a MDL of 4 ppbv was achieved for N_2O measurements.

For ambient CO and N_2O concentration measurements using a line-locking operational mode, an inlet tube of the QEPAS sensor was placed outside the laboratory and atmospheric air was pumped into the sensor. The results of continuous measurements of atmospheric CO and N_2O concentration levels for a 5 h period are shown in Fig. 21.6a, b, respectively. The highest CO concentration spikes are caused by cigarette smoke whereas all other less intense spikes, recorded on top of the CO atmospheric background of ~130 ppbv, are due to automobile emissions. The mean atmospheric concentration of N_2O was calculated to be 350 ppbv when using the P(41) N_2O line at 2,169.6 cm^{-1}. Due to a long atmospheric residence time, the N_2O concentration is well mixed in the lower atmosphere and therefore its atmospheric concentration level is relatively stable as can be seen from Fig. 21.6b.

21.5 QEPAS Based ppb-Level Detection of Nitric Oxide (NO) Detection

21.5.1 Motivation for NO Detection

The capability of detecting and quantifying nitric oxide (NO) at ppbv concentration levels has an important impact in diverse fields of applications including environmental monitoring, industrial process control and medical diagnostics. The major sources of NO emission into the atmosphere are associated with industrial combustion processes as well as automobile, truck, aircraft and marine transport emissions. Long term, continuous, reliable NO concentration measurements in ambient

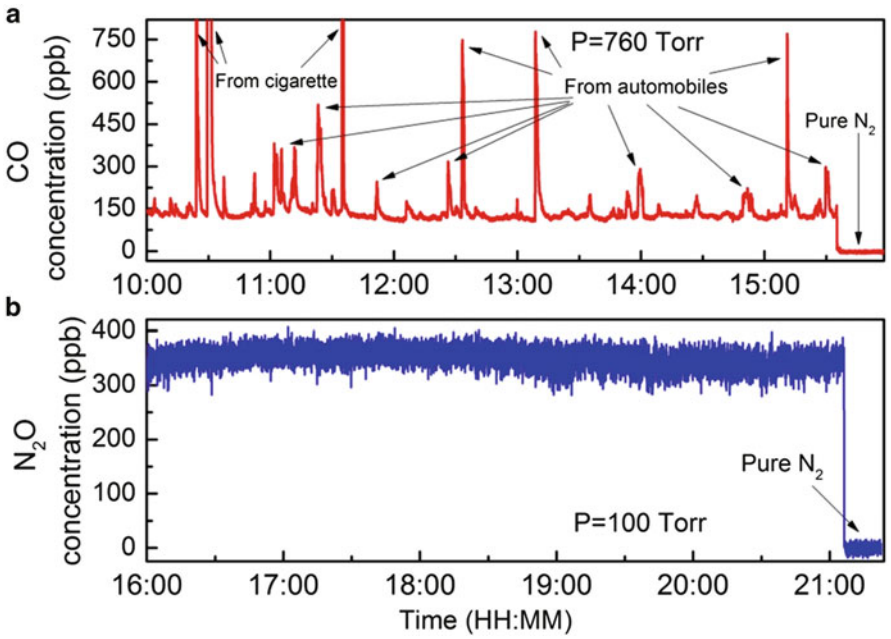

Fig. 21.6 Continuous monitoring of atmospheric CO and N_2O concentration levels from an air sampled on Rice University campus, Houston, TX, USA (Latitude and longitude are: 29° 43′ N/95° 23′ W). (**a**): CO concentration measurements; (**b**): N_2O concentration measurements

air are important because of NO's role in the depletion of earth's ozone layer and in the formation of acid rains and smog [14, 18].

21.5.1.1 CW TEC DFB-QCL Based QEPAS NO Sensor System

The QEPAS sensor for NO detection is similar to Fig. 21.1. In order to target the optimum H_2O and CO_2 interference-free NO doublet absorption lines centered at 1,900.08 cm^{-1} a 5.26 μm CW HHL packaged TEC DFB-QCL was used as an excitation source (see Fig. 21.7). The DFB-QCL emits ~100 mW optical power at an operating temperature and current of 22 °C and 890 mA, respectively. Similar to the CO QEPAS sensor the DFB-QCL current and temperature were set and controlled by a control electronics unit (CEU), which is also employed to modulate the laser current, to lock the laser frequency to the selected absorption line, and to measure the current generated by QTF in response to the photoacoustic signal. During the NO sensor evaluation test all the measurements were performed at a gas pressure of 250 Torr and modulation depth of 5 mA [7].

Similar to the CO QEPAS sensor the DFB-QCL current and temperature were set and controlled by a CEU, which is also employed to modulate the laser current, to lock the laser frequency to the selected absorption line, and to measure the current generated by QTF in response to the photoacoustic signal. During the NO

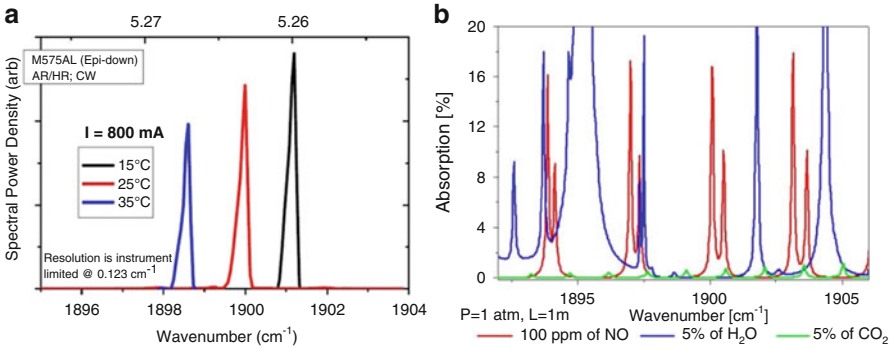

Fig. 21.7 (**a**) Emission spectra of 1,900 cm^{-1} TEC CW DFB QCL and (**b**) HITRAN simulated spectra of NO, H_2O, and CO_2

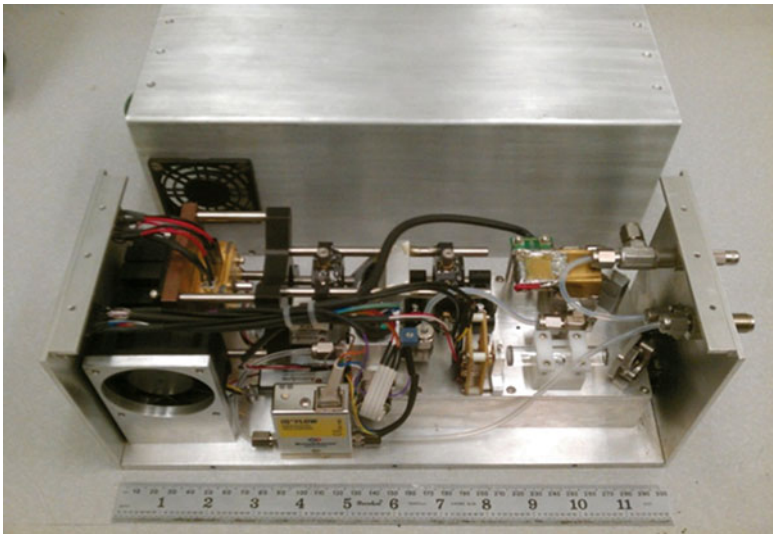

Fig. 21.8 Compact Prototype NO sensor

sensor evaluation test all the measurements were performed at a gas pressure of 250 Torr and modulation depth of 5 mA [7].

A photograph of a completed compact, autonomous DFB-QCL based WMS QEPAS NO platform enclosed in a 12.3×5.3×5.1 in. aluminum enclosure is shown in Fig. 21.8.

The 2*f* QEPAS signal amplitude when the DFB-QCL frequency is tuned across and locked to the NO doublet absorption line at 1,900.08 cm^{-1} is depicted in Fig. 21.9a, b, respectively. For a 95 ppbv of NO in N_2 calibrated mixture and 2.5 % water vapor concentration the calculated noise-equivalent (1σ) concentration of NO with a 1 s averaging time is 3 ppbv at gas pressure of 250 Torr. The corresponding absorption coefficient normalized to the detection bandwidth and optical power is 6.2×10^{-9} cm^{-1} $W/Hz^{1/2}$.

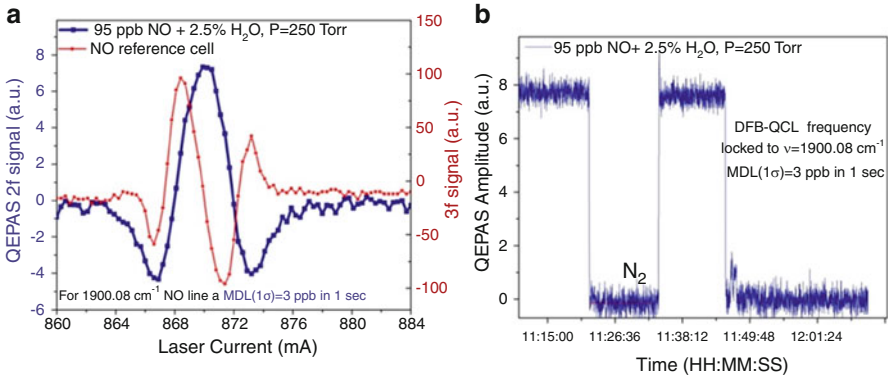

Fig. 21.9 *2f* QEPAS signal amplitude when QCL frequency is tuned across (**a**) and locked (**b**) to the NO doublet absorption line at 1,900.08 cm^{-1}

Similar to CO QEPAS sensor a long term stability of the NO sensor platform was also investigated by using an Allan variance analysis. From the Allan deviation plot the optimum averaging time for compact prototype NO QEPAS sensor is 200 s, what corresponds to an improved NO minimum detectable concentration of ~0.3 ppbv. For the purpose of environmental monitoring, where sensor time response is not a critical parameter, a 200 s averaging time can be normally utilized to allow a detection limit of NO below 1 ppbv.

21.6 Summary and Future Directions

This work focused on recent advances in the development of sensors based on infrared semiconductor lasers for the detection, quantification and monitoring of trace gas species and their applications in atmospheric chemistry and industrial process control. The development of compact trace gas sensors, in particular based on quantum cascade lasers permit the targeting of strong fundamental rotational-vibrational transitions in the mid-infrared, that are one to two orders of magnitude more intense than overtone transitions in the near infrared.

The architecture and performance of two sensitive, selective and real-time gas sensor systems based on mid-infrared semiconductor lasers was described. High detection sensitivity at ppbv and sub-ppbv concentration levels requires sensitivity enhancement schemes such as wavelength modulation and quartz-enhanced-photo-acoustic spectroscopy. These spectroscopic methods can achieve minimum detectable absorption losses in the range from 10^{-8} to 10^{-11} $cm^{-1}/\sqrt{Hz}$.

A QEPAS based sensor capable of ppbv level detection of CO, a major air pollutant, was developed. A 4.61 μm high power CW DFB QCL that emits a maximum optical power of >1 W in a continuous-wave (CW) operating mode [15] was used. Noise-equivalent sensitivity (NES, 1σ) of 2 ppbv was achieved at atmospheric pressure

with a 1 s. acquisition time targeting the R(6) CO line, located at 2,169.2 cm^{-1}. Furthermore, a QEPAS sensor for atmospheric NO detection using a high performance (>100 mW) 5.26 μm CW TEC DFB-QCL (mounted in a high heat load package) is reported. A 1σ minimum detection limit of 3 ppbv was achieved for a sampling time of 1 s. using an interference free NO absorption line located at 1,900.08 cm^{-1}[7, 8].

New target analytes such as SO_2, OCS, CH_2O, HONO, H_2O_2, C_2H_4 and other hydrocarbons are planned. Furthermore, monitoring of broadband absorbers such as acetone, acetone peroxide and UF_6 will be investigated. In addition, ultra-compact, low-cost robust sensor designs are being considered.

Acknowledgments The Rice University group acknowledges financial support from a National Science Foundation (NSF) grant EEC-0540832 entitled "Mid-Infrared Technologies for Health and the Environment (MIRTHE)", a NSF-ANR award for international collaboration in chemistry "Next generation of Compact Infrared Laser based Sensor for environmental monitoring (NexCILAS)" and grant C-0586 from the Robert Welch Foundation.

References

1. Faist J (2013) Quantum cascade lasers. Oxford University Press, Oxford. ISBN 13: 978-0198528241
2. Capasso F (2010) High-performance midinfrared quantum cascade lasers. SPIE Opt Eng 49:111102
3. Razeghi M, Bai Y, Slivkin S, Davish SR (2010) High-performance InP-based midinfrared quantum cascade lasers at Northwestern University. SPIE Opt Eng 49:111103-4
4. Lyakh A, Maulini R, Tsekoun AG, Patel CK (2010) Progress in high-performance quantum cascade lasers. SPIE Opt Eng 49:111105
5. Razeghi M (2009) High-performance InP-based Mid-IR quantum cascade lasers. IEEE J Sel Top Quantum Elect 15:941–951
6. Le QY, Bai Y, Bandyopadhyay N, Slivken S, Razeghi M (2010) Room-temperature continuous wave operation of distributed feedback quantum cascade lasers with watt-level power output. Appl Phys Lett 97:231119-1
7. Dong L, Spagnolo V, Lewicki R, Tittel FK (2011) Ppb-level detection of nitric oxide using an external cavity quantum cascade laser based QEPAS sensor. Opt Express 19:24037–24045
8. Spagnolo V, Kosterev AA, Dong L, Lewicki R, Tittel FK (2010) NO trace gas sensor based on quartz enhanced photoacoustic spectroscopy and external cavity quantum cascade laser. Appl Phys B 100:125–130
9. Kosterev AA, Bakhirkin YA, Curl RF, Tittel FK (2002) Quartz-enhanced photoacoustic spectroscopy. Opt Lett 27:1902–1904
10. Kosterev AA, Tittel FK, Serebryakov D, Malinovsky A, Morozov A (2005) Applications of quartz tuning fork in spectroscopic gas sensing. Rev Sci Instrum 76:043105
11. Curl RF, Capasso F, Gmachl C, Kosterev AA, McManus B, Lewicki R, Pusharsky M, Wysocki G, Tittel FK (2010) Quantum cascade lasers in chemical physics. Chem Phys Lett Frontiers Article 487:1–18
12. Dong L, Kosterev AA, Thomazy D, Tittel FK (2010) QEPAS spectrophones: design, optimization, and performance. Appl Phys B 100:627–635
13. Ma Y, Lewicki R, Razeghi M, Tittel FK (2013) QEPAS based ppb-level detection of CO and N2O using a high power CW DFB-QCL. Opt Express 21:1008–1019
14. Seinfeld JH, Pandis SN (1998) Atmospheric chemistry and physics: from air pollution to climate change. Wiley, New York

15. Ma Y, Lewicki R, Razeghi M, Tittel FK (2013) QEPAS based ppb-level detection of CO and N2O using a high power CW DFB-QCL. Opt Express 21:1008–1019
16. Li J, Parchatka U, Königstedt R, Fischer H (2012) Real-time measurements of atmospheric CO using a continuous-wave room temperature quantum cascade laser based spectrometer. Opt Express 20:7590–7601
17. Tao L, Sun K, Amir Khan M, Miller DJ, Zondlo MA (2012) Compact and portable open-path sensor for simultaneous measurements of atmospheric N2O and CO using a quantum cascade laser. Opt Express 20:28106–28118
18. Kasyutich VL, Holdsworth RJ, Martin PA (2008) Mid-infrared laser absorption spectrometers based upon all-diode laser difference frequency generation and a room temperature quantum cascade laser for the detection of CO, N2O and NO. Appl Phys B 92:271–279